

CHARACTERISTICS, EVOLUTION AND MECHANISMS OF THE SUMMER MONSOON ONSET OVER SOUTHEAST ASIA

ZUQIANG ZHANG,^{a,b,*} JOHNNY C. L. CHAN^a and YIHUI DING^b

^a *Laboratory for Atmospheric Research, Department of Physics and Materials Science, City University of Hong Kong, Hong Kong, People's Republic of China*

^b *Laboratory of Climate Study, National Climate Center, China Meteorological Administration, Beijing, People's Republic of China*

Received 24 November 2003

Revised 16 June 2004

Accepted 16 June 2004

ABSTRACT

Based on the 1979–95 mean pentad reanalysis data from the US National Centers for Environmental Prediction, the climatological characteristics and physical mechanism of the Asian summer monsoon (ASM) onset are investigated. Special focus is given to whether the ASM onset starts earlier over the Indochina Peninsula than over the South China Sea (SCS) and why the ASM is established the earliest over Southeast Asia.

An examination of the composite thermodynamic and dynamic quantities confirms that the ASM onset commences earliest over the Indochina Peninsula, as highlighted by active convection and rainfall resulting from the convergence of southwesterly flow from the Bay of Bengal (BOB) vortex and easterly winds associated with the subtropical anticyclone over the SCS. Two other important characteristics not previously noted are also identified: the earliest reversal of meridional temperature gradient throughout the entire troposphere and the corresponding establishment of an easterly vertical wind shear, which are due to upper level warming caused by eddy (convective) transport of latent heat.

These changes in the large-scale circulation suggest that, in addition to rainfall, a reversal in the planetary-scale circulation should be included in determining the timing of the ASM onset. With such a consideration, the climatological ASM onset occurs first over southeastern BOB and southwestern Indochina Peninsula in early May, and then advances northeastward to reach the SCS by the fourth pentad of May (16–20 May). The monsoon then covers the entire Southeast Asia region by the end of May. Subsequently, a similar onset process begins over the eastern Arabian Sea, India and western BOB, and the complete establishment of the ASM over India is accomplished in mid June. In the process of the onset of each ASM component, the reversal of the upper level planetary-scale circulation depends strongly on that of the meridional temperature gradient. Over the Indochina Peninsula, the seasonal transition of upper level temperature results from convection-induced diabatic heating, whereas over western Asia it is attributed to subsidence warming induced by the active ascending motion over the former region.

The steady increase in surface sensible heating over the Indian subcontinent and the latent heating over the tropical Indian Ocean in April to early May appear to be the major impetus for the development of the cyclonic vortex over the BOB. A similar enhancement over the Arabian Peninsula and the surrounding regions is also identified to be crucial to the development of the so-called onset vortex over the Arabian Sea, and then ultimately to the ASM onset over India. Copyright © 2004 Royal Meteorological Society.

KEY WORDS: South China Sea; Indochina Peninsula; Asian summer monsoon; rainfall

1. INTRODUCTION

Because of the importance of the Asian summer monsoon (ASM), a good documentation and understanding of its climatology is essential. Indeed, the time for the onset of various components of the ASM has long been of great interest (Ramage, 1971; Rao, 1976). Based on the investigation of previous scientists, Tao and Chen (1987) proposed various mean onset dates of the ASM over South Asia, East Asia and Southeast Asia, with

* Correspondence to: Zuqiang Zhang, Division of Climate Dynamics, National Climate Center, China Meteorological Administration, No. 46 Zhongguancun South Ave., Haidian District, Beijing 100081, China; e-mail: zhangzq@cma.gov.cn

the one over the South China Sea (SCS) region being the earliest in early to mid May. This statement became a major reason for the initiation of the SCS Monsoon Experiment (SCSMEX) in 1998 (Ding *et al.*, 1999; Lau *et al.*, 2000). Numerous studies have also been carried out to identify the onset date of the SCS summer monsoon (SCSSM) in the climate mean, as well as in individual years. While the climatological SCSSM onset occurs during the fourth pentad of May (Xie *et al.*, 1996; Yan, 1997; Li and Qu, 1999), a substantial interannual variability in the onset date exists. For example, Chan *et al.* (2000) analysed the SCSMEX datasets and suggested a delayed SCSSM onset on around 25 May in 1998.

However, Ananthakrishnan *et al.* (1981) pointed out that the summer monsoon onset over the southeast Bay of Bengal (BOB) starts towards the end of April, earlier than any land monsoon onset. Some recent studies have also suggested that the earliest onset of the ASM may not necessarily commence over the SCS. Indeed, heavy rainfall begins climatologically over the Indochina Peninsula in early May, about 10–15 days earlier than the SCS (Lau and Yang, 1997; Matsumoto, 1997; Webster *et al.*, 1998; Wu and Zhang, 1998; Wu and Wang, 2000). However, the occurrence of heavy rainfall during the seasonal transition period does not necessarily represent the ASM onset. For example, heavy rainfall is often observed in the southern coastal regions of China from late April to early May, which is referred to as the 'pre-summer rainy season over South China' by Chinese meteorologists (Ding, 1994), but the summer monsoon is still far from the onset at that time. Simply using rainfall and/or outgoing longwave radiation (OLR) to argue for the ASM onset first occurring over the Indochina Peninsula may, therefore, not be sufficient. In fact, the ASM onset is quite a complicated process that includes not only an abrupt increase in rainfall, but also a seasonal reversal of the large-scale ocean–land thermal contrast and the associated reversal of atmospheric circulation. Therefore, it seems reasonable to re-examine the ASM onset date from the physical mechanism perspective, i.e. by examining the dynamic and thermodynamic variations in the planetary circulation rather than only the rainfall or convection.

The physical mechanism responsible for the ASM onset is usually attributed to seasonal changes in the ocean–landmass thermal contrast. The seasonal transition of the atmospheric circulation over the mid and low latitudes of Asia in late spring or early summer is generally regarded as a result of the rapid warming of the Asian landmass (Murakami and Ding, 1982; Luo and Yanai, 1983; Krishnamurti, 1985; He *et al.*, 1987; Yanai *et al.*, 1992). As an elevated heat source in spring and summer, the role of the Tibetan Plateau in this transition has also attracted significant and continuous attention of meteorologists since the 1950s (Staff Member of Academia Sinica, 1957; Flohn 1957, 1960; Ye and Gao 1979; Luo and Yanai 1984). Based on the objectively analysed FGGE (First GARP (Global Atmospheric Research Program) Global Experiment) dataset, He *et al.* (1987) identified two successive stages of upper tropospheric warming over the eastern Tibetan Plateau in May and over the Iran Plateau in June, each of which is accompanied by a distinct seasonal transition of the atmospheric circulation. Yanai *et al.* (1992) indicated that diabatic heating over the eastern Tibetan Plateau accounts for the tropospheric warming there in the first transition, which leads to the reversal of the meridional gradient of temperature (MGT) and the establishment of low-level southwesterlies over the BOB. Li and Yanai (1996) suggested that such heating results mainly from sensible heating over the plateau in May and June. Yanai *et al.* (1992) further pointed out that adiabatic warming produced by strong subsidence in the upper troposphere is the dominant cause of the warming over the Iran Plateau, which was also illustrated clearly by Hsu *et al.* (1999).

The Tibetan Plateau is mainly located in the mid-latitudes, and so is the corresponding warming of the local upper troposphere found in these studies. However, the ASM onset commences first in the tropical region. Krishnamurti *et al.* (1981) and Chang and Chen (1995) showed the onset of the East Asian summer monsoon (EASM) to be closely associated with the generation, development and movement of a low-level cyclonic vortex over the tropical Indian Ocean. It is difficult to relate this range-limited mid-latitude heat source in the mid and upper mid-latitude troposphere to the formation of a low-latitude cyclone and the associated convection in the tropics during the ASM onset. Nevertheless, Wu and Zhang (1998) proposed the downstream advection of heating as a mechanism to explain how the heating over the Tibetan Plateau could lead to an onset of the summer monsoon over the SCS region earlier than that over India. Recently, Hsu *et al.* (1999) investigated characteristics of the large-scale circulation and heating during the first transition of the ASM. They found that the strongest diabatic heating averaged within 90–110°E appears over the sloping

terrain south of the Tibetan Plateau rather than exactly on top, which implies that the Tibetan Plateau is unlikely to be the sole and most important factor for the first transition of the ASM. In a recent study, Xu and Chan (2001) showed that the MGT reversal in the upper troposphere (500–200 hPa) within (27.5–37.5°N, 5–20°E), which Ueda and Yasunari (1998) considered to be the fundamental factor for the ASM onset over Southeast Asia, did not occur until mid June over the longitudes of the central Tibetan Plateau and the BOB. These studies suggested that the influence of the Tibetan Plateau as a heat source on the ASM onset may be over-emphasized and that other mechanisms may not have been identified. In other words, the physical processes of the ASM onset in tropical Asia have not been completely identified, especially for its early stage before mid May when the thermal forcing of the Tibetan Plateau remains unremarkable.

The objectives of the present study are: (1) to examine the evolution of the climatological features of the general circulation during the seasonal transition in the Asian monsoon regions, with a view to identifying the causes of the intense rainfall over the Indochina Peninsula in early May; (2) to document the advance of the ASM onset in the tropical Asian monsoon region; and (3) to estimate the roles of surface heat fluxes at low latitudes on the ASM onset. The data and methods used in this study are described in Section 2. Seasonal transition characteristics of the lower and upper level atmospheric circulation are first discussed in Section 3. The advance of the ASM onset in the tropical Asian monsoon region is then investigated in Section 4. The role of surface heat fluxes over the monsoon regions on the ASM onset is examined in Section 5. The results from these three sections will be used to formulate a hypothesis on the physical processes involved in the entire ASM onset process, which is presented in Section 6, together with the summary and discussion.

2. DATA AND METHODOLOGY

2.1. Data

The principal dataset used in this study is the daily mean global atmospheric data provided by the National Centers for Environmental Prediction–National Center for Atmospheric Research reanalysis (Kalnay *et al.*, 1996). All the climatological pentad means in this study are constructed from the daily means for the period 1979–95. The wind, geopotential height, vertical velocity, temperature and specific humidity data have a horizontal resolution of 2.5° latitude square at 17 standard pressure levels. Surface heat fluxes are on a Gaussian grid of T62 with a horizontal resolution of ~1.9° latitude square. The climatological pentad mean OLR data on 2.5° latitude square grids with global coverage are obtained from pentad means of the National Oceanic and Atmospheric Administration satellite observations spanning from 1979 to 1995. The Climate Prediction Center Merged Analysis of Precipitation (CMAP) of pentad mean climatology for the same period is also employed in this study.

Relevant parameters are composited in this study. In addition to the examination of the various fundamental quantities, further diagnoses on the spatial and temporal variations of these quantities, as well as the heat budgets, are made based on the methodology described in Section 2.2.

2.2. Methodology

The apparent heat source Q_1 and the apparent moisture sink Q_2 (e.g. Yanai *et al.*, 1973, 1992) are computed from

$$Q_1 = C_p \left(\frac{p}{P_0} \right)^\kappa \left(\frac{\partial \theta}{\partial t} + \vec{V} \cdot \nabla \theta + \omega \frac{\partial \theta}{\partial p} \right) \quad (1)$$

and

$$Q_2 = -L \left(\frac{\partial q}{\partial t} + \vec{V} \cdot \nabla q + \omega \frac{\partial q}{\partial p} \right) \quad (2)$$

where θ is the potential temperature, \vec{V} is the horizontal velocity vector, ω is the vertical velocity in p -coordinates, p is the pressure, q is the specific humidity, $\kappa = R/C_p$, with R and C_p being the gas constant

and the specific heat at constant pressure of dry air respectively, $P_0 = 1000$ hPa, L is the latent heat of condensation, and ∇ is the isobaric gradient operator.

The residuals of heat and moisture budgets of the resolvable motion are Q_1 and Q_2 , and may be interpreted as

$$Q_1 = Q_R + L(c - e) - \frac{\partial \overline{s'\omega'}}{\partial p} \quad (3)$$

and

$$Q_2 = L(c - e) + L \frac{\partial \overline{q'\omega'}}{\partial p} \quad (4)$$

where Q_R is the radiative heating rate, c is the rate of condensation per unit mass of air, e is the rate of re-evaporation of cloud and rainwater, $s = C_p T + gz$ the dry static energy, and T the temperature. The prime denotes the deviation from the average due to unresolved eddies, such as cumulus convection and turbulence.

According to Equations (3) and (4), Q_1 consists of radiational heating, latent heat release and vertical heat transport by cumulus- and turbulence-generated eddies, and Q_2 includes the net condensation of moisture and vertical moisture transport by cumulus- and turbulence-induced eddies. In the case of active convection, the effects of vertical heat transfer by eddies are so pronounced that the maximum in Q_1 usually shifts to a higher level than that of Q_2 . Because of this, the vertical heat transfer of eddies can be easily detected through the comparison of vertical cross-sections or profiles of Q_1 and Q_2 (Yanai *et al.* 1973, 1992; Luo and Yanai 1984).

To determine the climatological evolution of different variables in each pentad, the temporal or spatial changes of each variable X are calculated as follows:

$$\text{Temporal : } \Delta X(P) = X(P) - X(P - 1) \quad (5)$$

$$\text{Spatial : } \Delta X(J) = X(J) - X(J - 1) \quad (6)$$

where J is the grid number in either the zonal or meridional direction and P is the pentad number. In this study, meridional gradients of all the variables are calculated according to Equation (6).

3. EVOLUTION OF THE ASM

3.1. Low-level flow and cyclonic vortices

As reported by many previous studies (Krishnamurti *et al.*, 1981; Chang and Chen 1995; Xie *et al.*, 1996; Chan *et al.*, 2000), the low-level cyclonic vortex over the tropical Indian Ocean plays a significant role in the establishment of a steady and intense southwesterly flow over the BOB and the SCS prior to the ASM onset. Therefore, the development of the low-level cyclonic vortex and related flows is investigated first.

To highlight the characteristics of the low-level flow pattern prior to the monsoon onset, pentad mean distributions of winds and the time rate of change of relatively vorticity (calculated using Equation (5), but over the specified period) are computed for two periods, 26 April–10 May and 26 May–10 June, which are considered as the crucial time intervals for the ASM onset over the Indochina Peninsula and India respectively (Lau and Yang, 1997; Wu and Wang, 2000). Prior to the monsoon onset over the former region, enhancements of cyclonic vorticity are found along the coast of Arabian Peninsula, BOB and the region from southern Indochina Peninsula to the northern part of the SCS (Figure 1(a)). To the south of each positive centre, a centre of opposite sign is found in the equatorial band. The westerly flow over the equatorial eastern Indian Ocean between the two vortices appears to converge with the southeasterlies from the SCS over the southern Indochina Peninsula. Note that the western Pacific subtropical high (WPSH) still occupies the SCS, and an easterly component prevails over the 5–15°N band of the Arabian Sea. This pattern suggests that

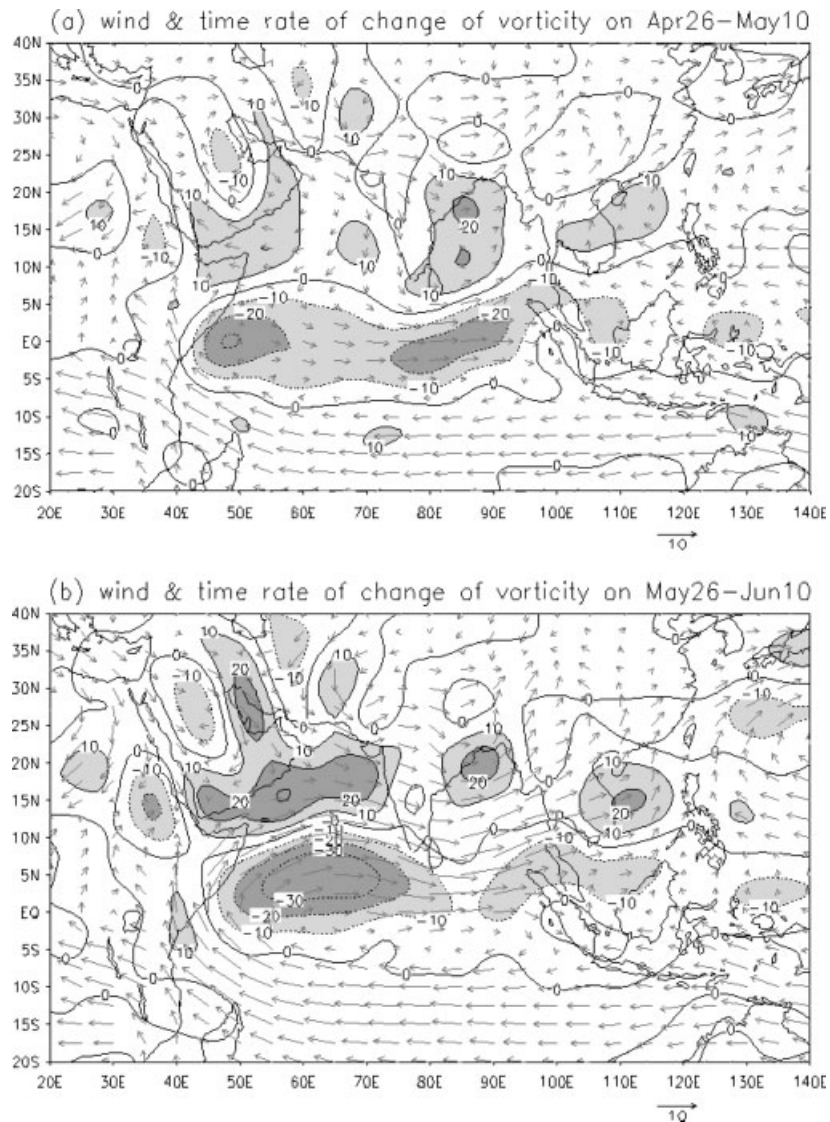


Figure 1. Mean 850 hPa wind (arrows, m s^{-1}) and time rate of change of relative vorticity (contours, 10^{-7} s^{-1} per pentad) in each pentad of the periods from (a) 26 April to 10 May and (b) 26 May to 10 June. Light and dark shadings indicate the absolute value of the time rate of change of relative vorticity $> 10 \times 10^{-7} \text{ s}^{-1}$ per pentad and $> 20 \times 10^{-7} \text{ s}^{-1}$ per pentad respectively

only the low-level dynamic condition over the southern Indochina Peninsula is ready for the monsoon onset at this time.

Compared with the distribution of wind and time rate of change of vorticity over the western Indian Ocean in Figure 1(a), a similar but stronger pattern is found over the Arabian Sea and western equatorial Indian Ocean 1 month later (Figure 1(b)). Consistent with the increasing vorticity, the Somalia cross-equatorial flow is established off the east coast of Africa, which turns into westerlies over the northern Indian Ocean, suggesting the impending monsoon onset over India.

The results from Figure 1 suggest that the development of cyclonic vorticity and the associated westerlies are chiefly confined to the $5\text{--}20^\circ\text{N}$ band. As such, this latitude band is chosen to examine the time evolution of other atmospheric variables in the following subsections.

3.2. Low-level zonal wind and stability

Using Equation (5), the pentad mean time rates of change of relative vorticity and 850 hPa winds in each pentad are obtained (Figure 2(a)). Apparently, cyclonic vorticity first increases over eastern India in early March, and then over the western BOB in April. Afterwards, its time rate of change increases to $\sim 10 \times 10^{-7} \text{ s}^{-1}$ per pentad till the end of May. A corresponding positive tendency in the southwesterly (northwesterly) component is observed east (west) of the largest increase in cyclonic vorticity (about 85°E). The increase in the southwesterly component extends from the BOB to the Indochina Peninsula and then to the SCS in mid April. A similar development is also found over $40\text{--}60^\circ\text{E}$, but is delayed by about half a month. From early May, westerly winds increase with time over the entire $40\text{--}140^\circ\text{E}$ domain, which suggests the initiation of the seasonal transition in the entire Asian tropical region.

The westerly wind appears first over India and the BOB around mid April, with northwesterly and southwesterly flows west and east of 85°E respectively (Figure 2(b)). This suggests that the seasonal transition of the low-level wind over this region in April is associated with the development of the cyclonic vortex shown both in Figures 1(a) and 2(a). With the intensification of the southwesterly component from the BOB and Indochina Peninsula, the easterly component over the SCS retreats to east of 120°E on 20–25 May, indicative of the retreat of the WPSH from the SCS, which has been considered as a precondition for the SCSSM onset.

The evolution of the saturated equivalent potential temperature (SEPT, θ_{SE}) seems to be related to that of the low-level wind. As early as the beginning of April, the Indochina Peninsula becomes the warmest and most moist region with a large value of $\theta_{\text{SE}} > 335 \text{ K}$, which is mainly due to the southeasterly flow of the WPSH from the western Pacific and the SCS that brings moisture to this region. At this time, the SCS is relatively dry until the eastward extension of the southwesterlies from the BOB into the Indochina Peninsula in late April and then into the SCS in mid May. In contrast, the relationship between low-level wind and θ_{SE} west of the BOB seems to be weaker, although the sudden increase of $\theta_{\text{SE}} > 335 \text{ K}$ over $75\text{--}90^\circ\text{E}$ in early June is likely related to the moisture transport by the Somalia cross-equatorial flow.

To investigate the effect of thermodynamic processes on the monsoon onset, a stability parameter of the atmosphere $\Delta\theta_{\text{SE}}$ can be defined:

$$\Delta\theta_{\text{SE}} = \theta_{\text{SE}}(1000 - 700 \text{ hPa}) - \theta_{\text{SE}}(600 - 300 \text{ hPa})$$

Positive values of $\Delta\theta_{\text{SE}}$, therefore, imply a decrease in θ_{SE} with height, and hence instability. It is apparent from Figure 2(c) that the troposphere over the Indochina Peninsula first becomes unstable in early March and reaches a maximum in early April. However, active convection, defined as $\text{OLR} < 235 \text{ W m}^{-2}$, does not occur there until the arrival of the southwesterlies from the BOB around 20 April (see Figure 2(b)). Afterwards, both the area of active convection and of $\Delta\theta_{\text{SE}} < -2.5 \text{ K}$ suddenly expand eastward to the entire SCS on 16–20 May, indicating the SCSSM onset. A similar distribution also occurs over the BOB. Around early June, areas of active convection and instability appear over India.

3.3. Upper level flow and geopotential height

The most significant upper level circulation over the Asian continent in summer is the extensive South Asia high (SAH) in the mid-latitudes and its associated strong easterlies over southern Asia. The evolution of the 200 hPa flow and the meridional gradient of geopotential height (MGGH) at this level from 16 April to 10 June are, therefore, investigated to examine the seasonal transition in the upper troposphere. Here, Equation (6) is applied in the calculation of MGGH, with the northern boundary of positive MGGH representing the ridge axis.

It appears that the seasonal evolution of the upper level winds and the SAH are different at different longitudes. During 16–20 April (Figure 3(a)), both the easterlies and positive MGGH east of 100°E have expanded northward as far as 10°N , while west of 80°E they are still confined to the south of 5°N . At this time, the strongest MGGH is observed over Sumatra and the Andaman Sea. In the subsequent several pentads (Figure 3(b)–(d)), both the ridge axis and the easterlies advance poleward along the so-called land bridge,

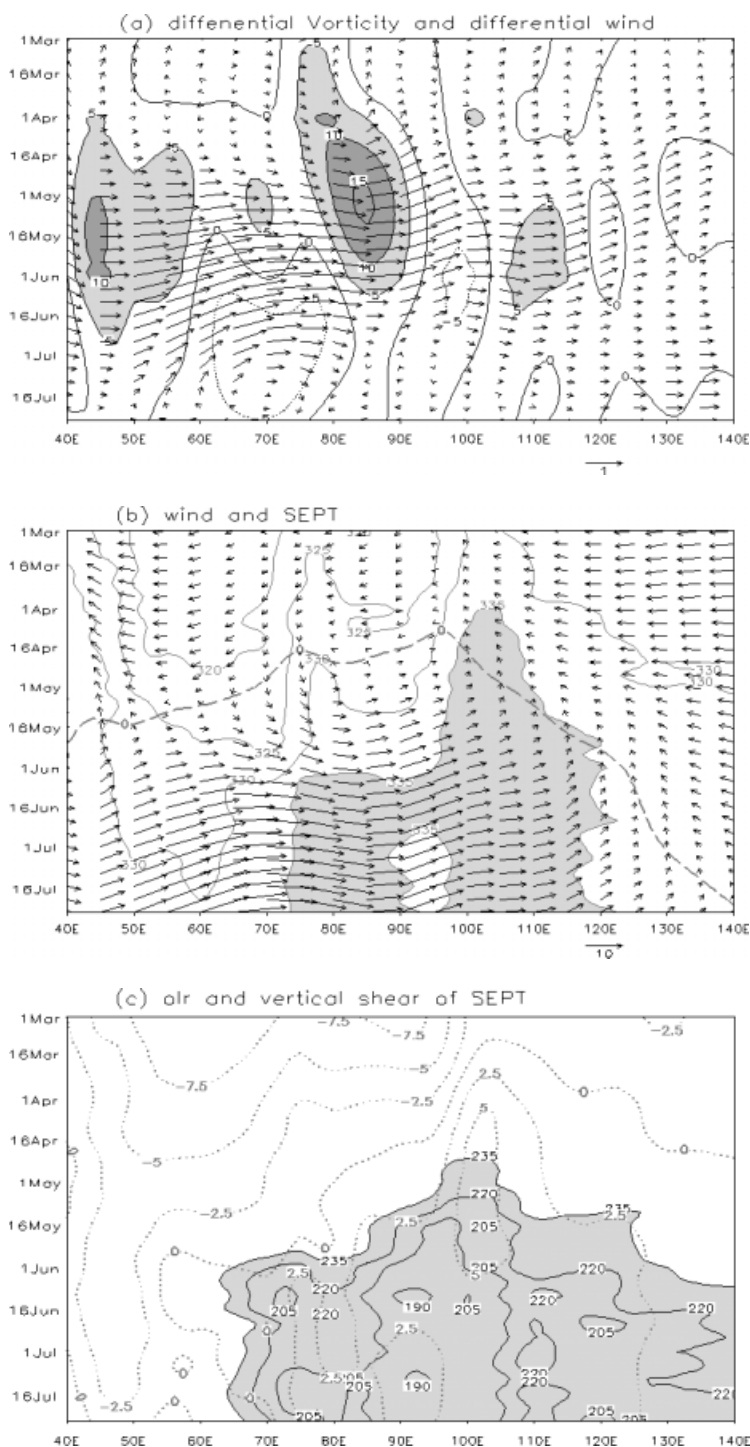


Figure 2. Longitude–time cross-sections of 5–20°N pentad mean variables. (a) Time rate of change of 850 hPa wind (arrows, m s^{-1}) and of relative vorticity (contours, 10^{-6} s^{-1}) in each pentad. Light and dark shadings indicate the change of relative vorticity in each pentad $> 5 \times 10^{-7} \text{ s}^{-1}$ and $> 10 \times 10^{-7} \text{ s}^{-1}$. (b) Pentad mean wind (arrows, m s^{-1}) and θ_{SE} (contours, K) at 850 hPa. Shaded areas indicate $\theta_{\text{SE}} > 335 \text{ K}$. The zero line of zonal wind is highlighted by a dashed line. (c) OLR (shaded, W m^{-2}) and vertical gradient of θ_{SE} (dotted lines, K) computed by the subtraction of θ_{SE} within 600–300 hPa from that of 1000–700 hPa. Only values of $\text{OLR} < 235 \text{ W m}^{-2}$ are shown

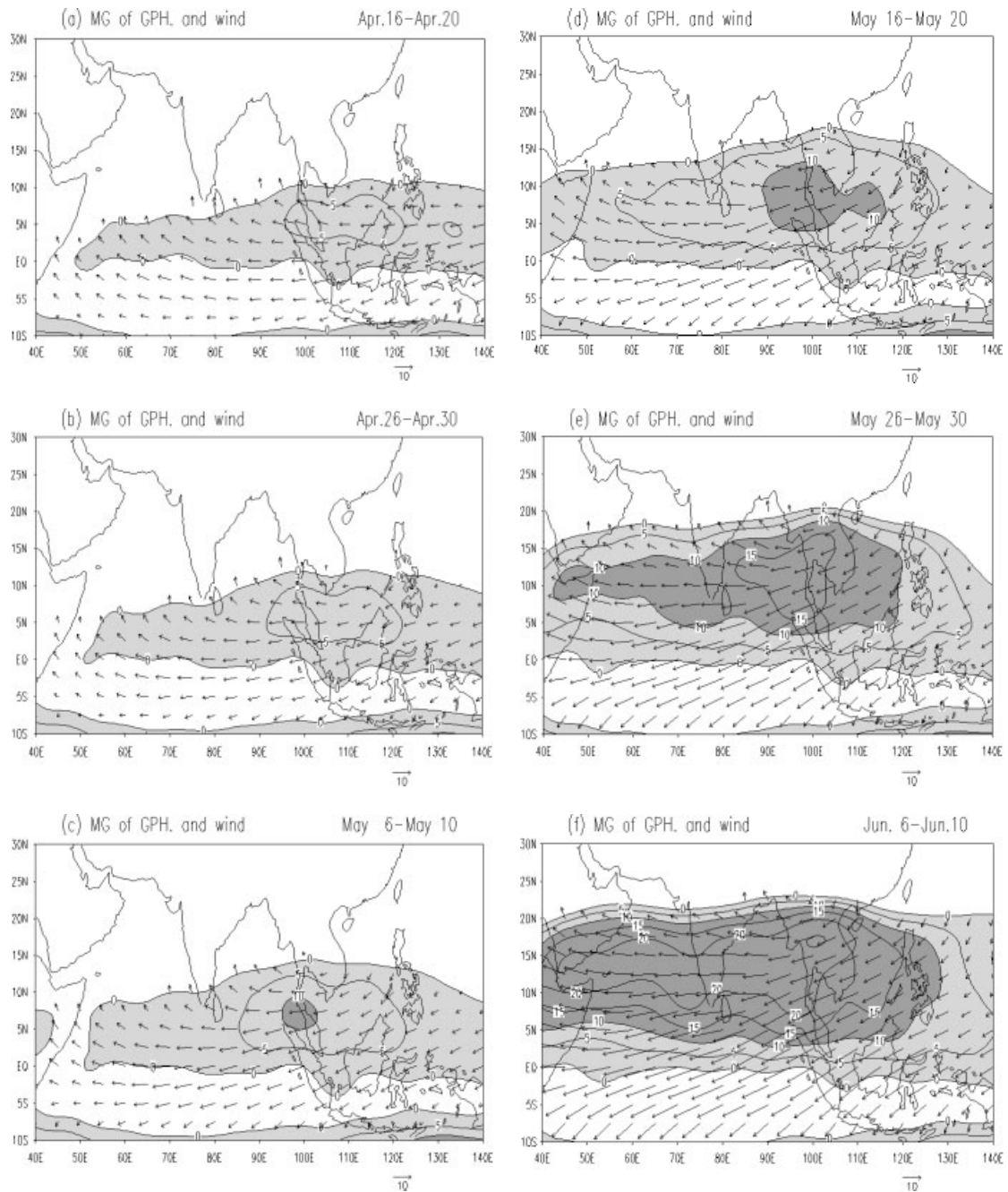


Figure 3. MGGH (contours, 10 gpm per 2.5° lat) and wind (arrows, m s^{-1}) at 200 hPa. Light and dark shadings indicate the values of MGGH per 2.5° lat > 0 and > 100 gpm respectively. Only the winds with an easterly component and positive values of MGGH are presented

reaching the northern part of the Indochina Peninsula by 16–20 May. Concurrently, the original MGGH maximum over Sumatra strengthens gradually and expands latitudinally in both directions. Finally, the area of positive MGGH and its associated easterly flow are established over the entire Indian subcontinent and the Arabian Sea during late May to early June (Figure 3(e) and (f)). Such an evolution demonstrates that, in the

upper troposphere, the monsoon-related seasonal transition occurs over the Indochina Peninsula earlier than over the other regions.

3.4. Upper level meridional gradient of temperature

Another characteristic of the seasonal transition in the Asia monsoon region is the reversal of wintertime negative MGT in the entire troposphere. At the end of April, positive MGT is confined to below 700 hPa and west of the central Indochina Peninsula (105°E), with maxima over India and the Arabian Peninsula (Figure 4(a)). In the upper troposphere, only a slight reversal of the MGT is observed over the BOB and the Indochina Peninsula, and westerly winds prevail over the entire region. In the following pentads, the area of positive MGT at the upper levels expands and extends downward with time, and finally merges with the one in the lower troposphere in mid May (Figure 4(b) to (d)). This result again suggests that the reversal of the MGT from negative to positive in the entire troposphere is accomplished first over the Indochina Peninsula and initiated from the upper troposphere. Meanwhile, associated with the reversal of the MGT over the Indochina Peninsula, the original westerlies in the upper troposphere are gradually replaced by easterlies.

The area of positive MGT and the easterly winds at the upper levels then extend both eastward and westward, and cover the entire domain by 1–5 June (Figure 4(e)–(h)). However, contrary to the situation over the Indochina Peninsula, the reversal of the MGT in the upper troposphere west of 70°E lags the appearance of easterly flows, which implies that the mechanism responsible may be different for these two regions. This issue will be addressed in Section 3.5.

To illustrate further the relationship between the transitions of the MGT and upper level zonal winds, their time evolutions over India, the Indochina Peninsula and the SCS are compared (Figure 5). Without exception, the switching of westerlies to easterlies in the upper troposphere agrees very well with the reversal of the MGT, which implies that the development of upper level easterlies in the Asian tropical monsoon regions depends strongly on the variation of the MGT. In fact, the mean positive MGT over 5–20°N and the associated positive MGGH imply that the core of upper level warming is mainly located to the north of this latitudinal band. As a response to the variation of MGGH, the reversal of wintertime westerlies to summertime easterlies in the upper troposphere occurs over this band.

3.5. Upper level diabatic heating

Longitude–pressure cross-sections of Q_1 and Q_2 are examined to determine the nature of the heating process responsible for the seasonal transition of the MGT in the Asian monsoon region (Figure 6). Prior to and during the onset over the Indochina Peninsula (26 April–20 May), the major difference in the vertical profiles of Q_1 and Q_2 is that Q_1 is strongest in the middle and upper troposphere, whereas the maximum Q_2 is found mainly in the lower troposphere (Figure 6(a) and (b)). Following the discussion in Section 2, this low-level maximum of Q_2 comes primarily from the latent heat of condensation released through active convection, whereas the vertical heat transport of cumulus- and turbulence-generated eddies accounts for the much stronger Q_1 at the middle and upper levels. This is why the positive MGT appears concurrently at the upper and lower levels, but extends downward from the upper troposphere and then merges with the one at the low levels (see Figure 4).

A similar enhancement of diabatic heating is found over the eastern Arabian Sea and India prior to and during the onset over India (21 May–15 June); but, west of 60°E, a cooling still remains (Figure 6(c) and (d)), which is presumed to be the reason for the delayed reversal of the MGT compared with that of the zonal wind (see Figure 4(e)–(g)). In addition, it also indicates that the reversal of the upper level MGT west of 60°E results from mechanisms other than the upward transport of the diabatic heating by cumulus- or turbulence-induced eddies. The diabatic cooling there actually prevents the MGT from reversing over the Arabian Peninsula and its surrounding regions. A detailed discussion on the mechanisms responsible will be given in Section 4.

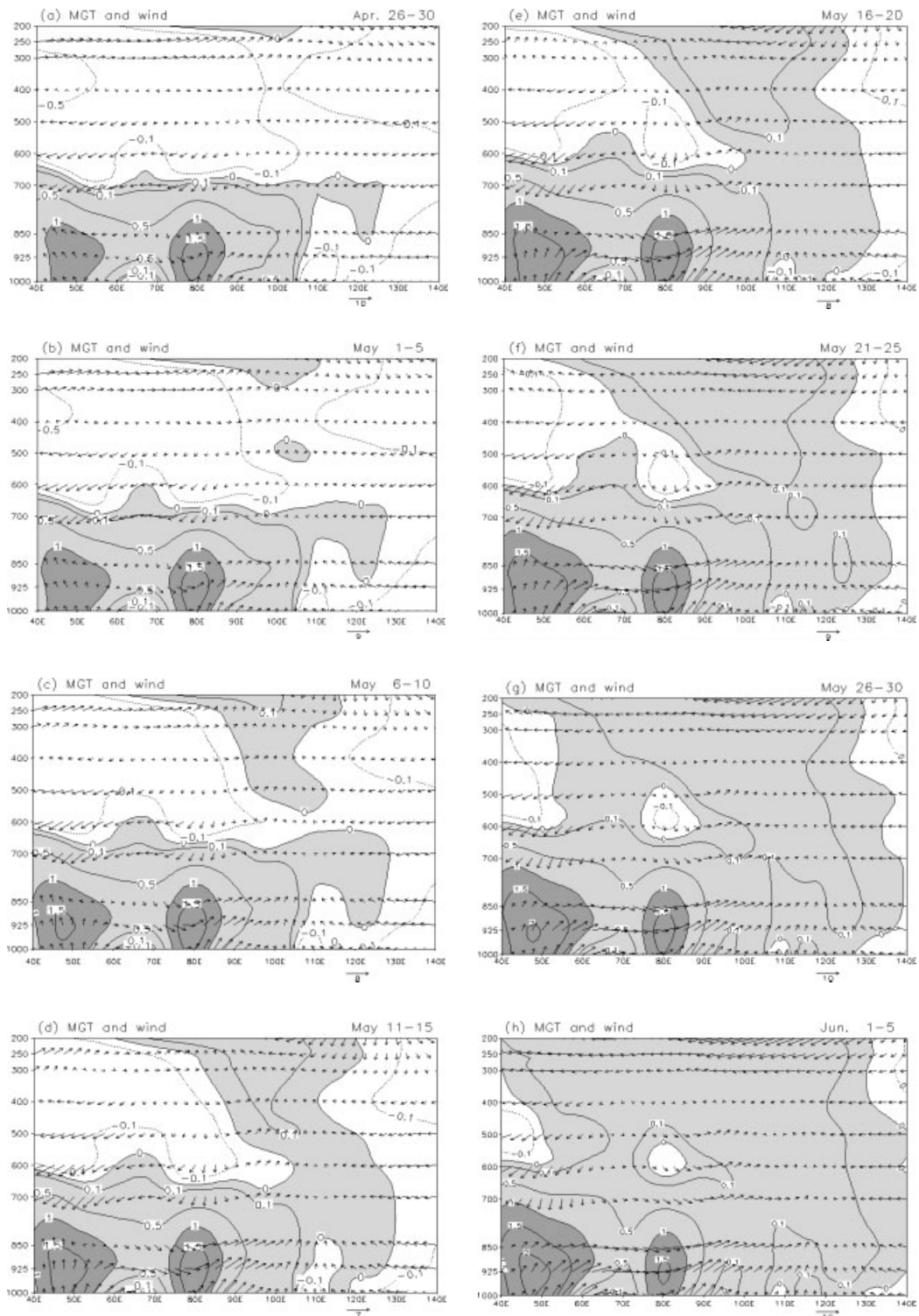


Figure 4. Longitude–pressure cross-sections of pentad mean MGT (contours, $^{\circ}\text{C}$ per 2.5° lat) and wind (arrows, m s^{-1}) over $5\text{--}20^{\circ}\text{N}$ from (a) 26–30 April to (h) 1–5 June in sequence. Light and dark shadings denote MGT per 2.5° lat $> 0^{\circ}\text{C}$ and $> 1^{\circ}\text{C}$ respectively. The contour or $\pm 0.1^{\circ}\text{C}$ per 2.5° lat is shown in particular

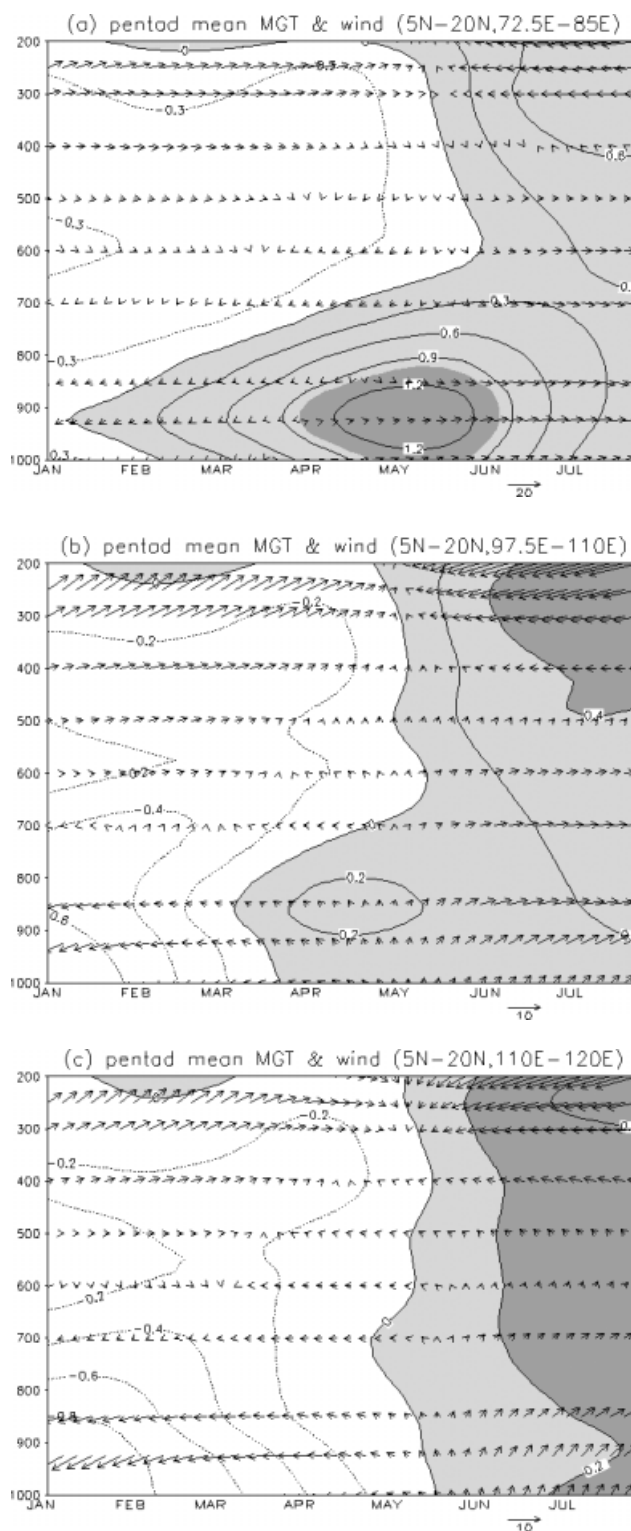


Figure 5. Time–pressure cross-sections of pentad mean MGT (contours, °C per 2.5° lat) and wind (arrows, m s⁻¹) over (a) 5–20°N, 72.5–85°E, (b) 5–20°N, 97.5–110°E and (c) 5–20°N, 110–120°E. Note the dark shadings in different panels are different. Right (upward)-directed arrows indicate westerly (southerly) wind, and vice versa

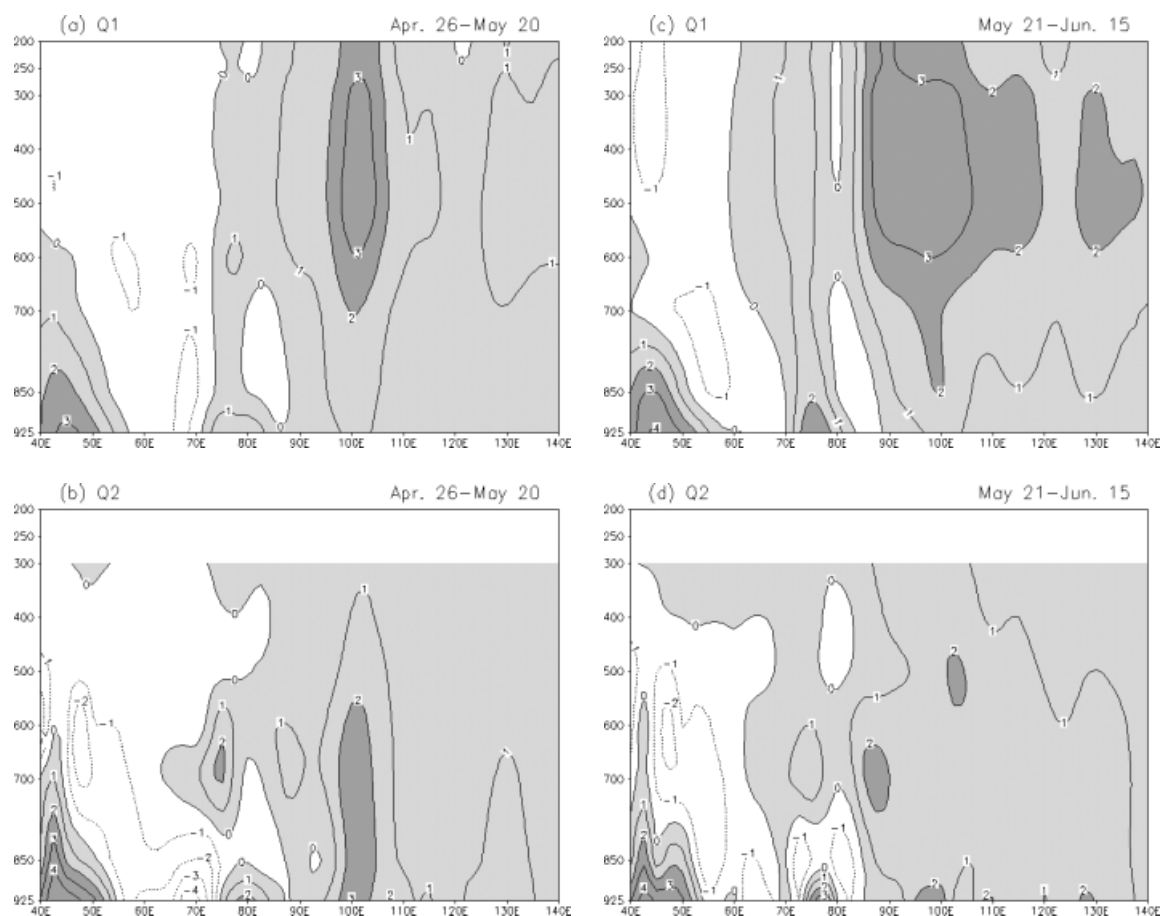


Figure 6. Longitude–pressure cross-sections of (a), (c) pentad mean apparent heat source Q_1 ($^{\circ}\text{C day}^{-1}$) and (b), (d) the apparent moisture sink Q_2 ($^{\circ}\text{C day}^{-1}$) over $5\text{--}20^{\circ}\text{N}$ during the period of 26 April to 20 May (left column) and 21 May to 15 June (right column). These two special periods are chosen to represent the distribution of Q_1 and Q_2 during the monsoon onset over the Indochina Peninsula and India respectively. Light and dark shadings denote the values $>0^{\circ}\text{C day}^{-1}$ and $>2^{\circ}\text{C day}^{-1}$.

3.6. Upper level adiabatic warming

Since the contribution from Q_1 apparently cannot explain the upper level MGT reversal in the area west of 60°E , the alternative must come from subsidence warming. Indeed, a close relationship exists between the vertical motion and temperature change at the upper levels in this area (Figure 7). Here, the domain of $27.5\text{--}37.5^{\circ}\text{N}$, $30\text{--}60^{\circ}\text{E}$ is chosen to highlight this relationship. A similar, but weaker, result is also obtained if the domain is extended southward to 20°N . The upper level warming and sinking motion start to increase from early May and reach a maximum around late May to early June, exactly prior to the monsoon onset over India. Hence, it is reasonable to assume that subsidence warming over the Iranian desert and its adjacent landmass is responsible for the enhancement of the MGGH and associated easterly winds in the upper troposphere.

To investigate the origin of the upper level subsidence flow over the desert regions in West Asia, the evolution of the 200 hPa velocity potential and divergent wind before, during and after the monsoon onset over Southeast Asia is examined (Figure 8). With the monsoon onset over there, an increasing intensification of upper level convergence takes place and gradually shifts poleward from the southern Arabian Peninsula. This means that the upper level subsidence over the desert regions of West Asia in May originates mostly from the monsoon-induced ascending motion over the Indochina Peninsula and the SCS, which agrees well with Hsu *et al.* (1999). In other words, the ASM onset over India and the Arabian Peninsula, to a large extent,

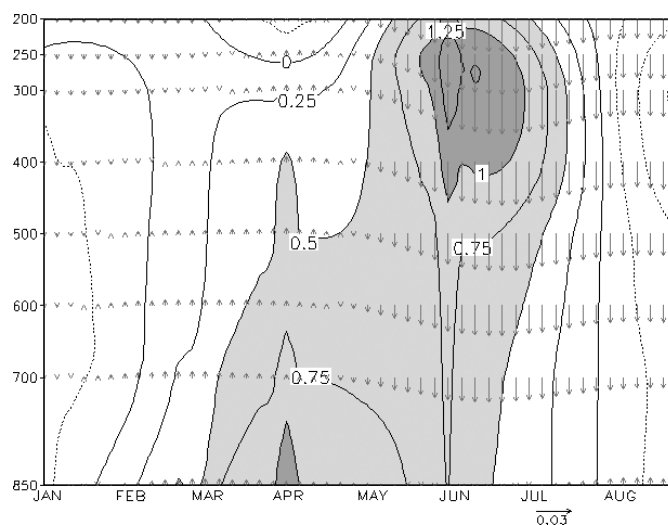


Figure 7. Pressure–time cross-section of vertical velocity (arrows, hPa s^{-1}) and time rate of change of air temperature in each pentad ($^{\circ}\text{C}$ per pentad) over $27.5\text{--}37.5^{\circ}\text{N}$, $30\text{--}60^{\circ}\text{E}$. Light and dark shadings indicate the value $>0.5^{\circ}\text{C}$ and $>1^{\circ}\text{C}$ per pentad respectively. The upward (downward) arrows represent ascending (descending) motion

depends on the monsoon onset over the BOB and the SCS, which may explain why the monsoon onset over India occurs later than the other two regions.

4. ADVANCE OF THE ASM

4.1. Nature of rainfall over the Indochina Peninsula

Heavy rainfall is generally observed over the Indochina Peninsula at the beginning of April, or even earlier. Meanwhile, another subtropical frontal rain belt is usually set up over southern China. The latter is likely due to the convergence of cold air from the mid-latitudes of East Asia and the moist southwesterly flow from the WPSH (e.g. Chang and Chen, 1995). Although these rainfall belts often merge, their nature is not necessarily the same.

In the first pentad of May, besides the heavy rainfall over Sumatra and Kalimantan Island, another centre of precipitation of $>6 \text{ mm day}^{-1}$ is found over southern China (left column of Figure 9). Notice that these two centres are connected to form a northeast–southwest-oriented rain belt through the Indochina Peninsula.

To determine possible differences in the nature of rainfall in these two areas, the low-level winds, atmospheric stability and upper level diabatic heating are examined. First of all, positive values of $\Delta\theta_{\text{SE}}$ are primarily confined to south of 25°N on 1–5 May, with the largest value over the Indochina Peninsula and negative values over the southeast coast of China (middle column of Figure 9). This pattern suggests much greater potential for the development of heavy convection over the Indochina Peninsula than over southern China, whereas the atmosphere over the coast of southeastern China remains stable. Consistently, in the right column of Figure 9, a strong diabatic heating over $\sim 3^{\circ}\text{C day}^{-1}$ occurs firstly over Indochina Peninsula, Sumatra and Kalimantan, but a relatively weak one is found over southern China. As the seasonal transition progresses, the upper level diabatic heating over southern China increases gradually, and reaches $\sim 3^{\circ}\text{C day}^{-1}$ by 16–20 May.

The different evolutions of atmospheric stability and upper level diabatic heating over the Indochina Peninsula and southern China suggest that, in early May, the rainfall over the former region originates from active cumulus convection, whereas that over the latter area is likely from the cold airmass from mid and higher latitudes of East Asia. Afterwards, the contribution of active cumulus convection to the rainfall over southern China gradually increases with time. Owing to the different nature of the rainfall, the associated

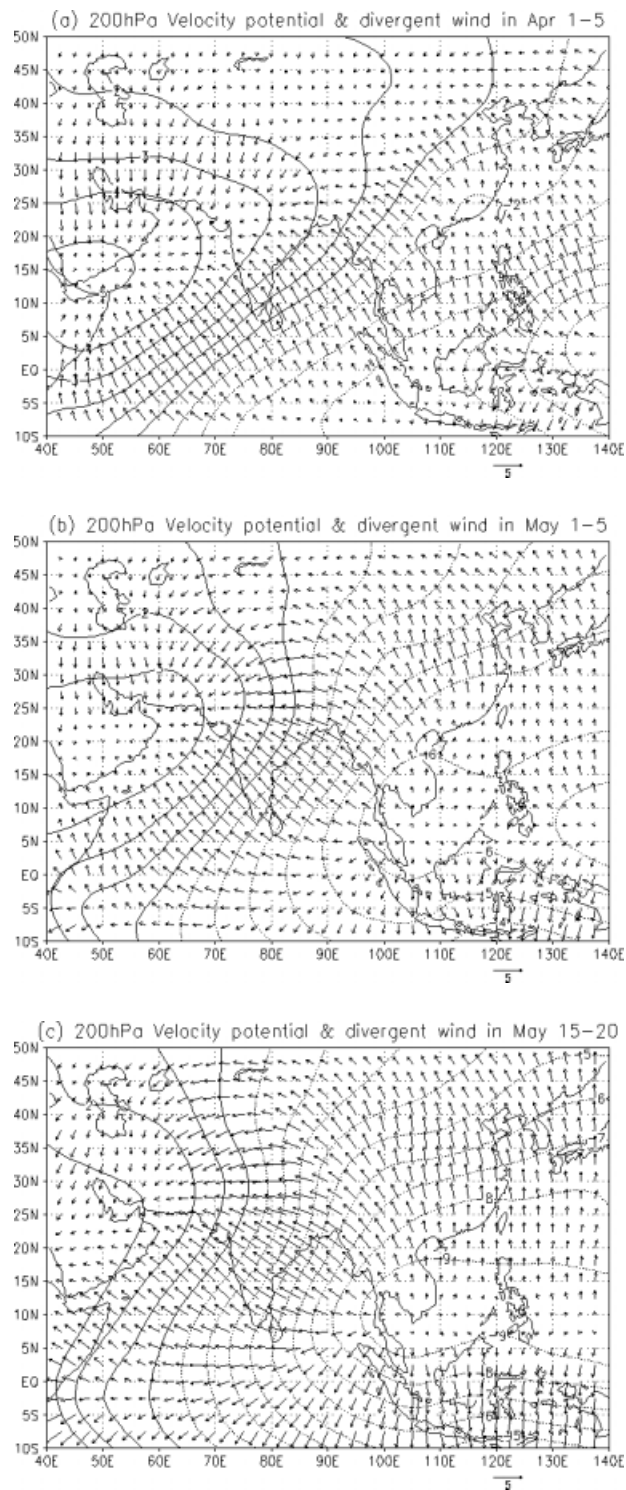


Figure 8. Evolutions of pentad-mean 200 hPa velocity potential (10^6 s^{-1}) and divergent wind (m s^{-1}) for (a) 1-5 April, (b) 1-5 May and (c) 15-20 May

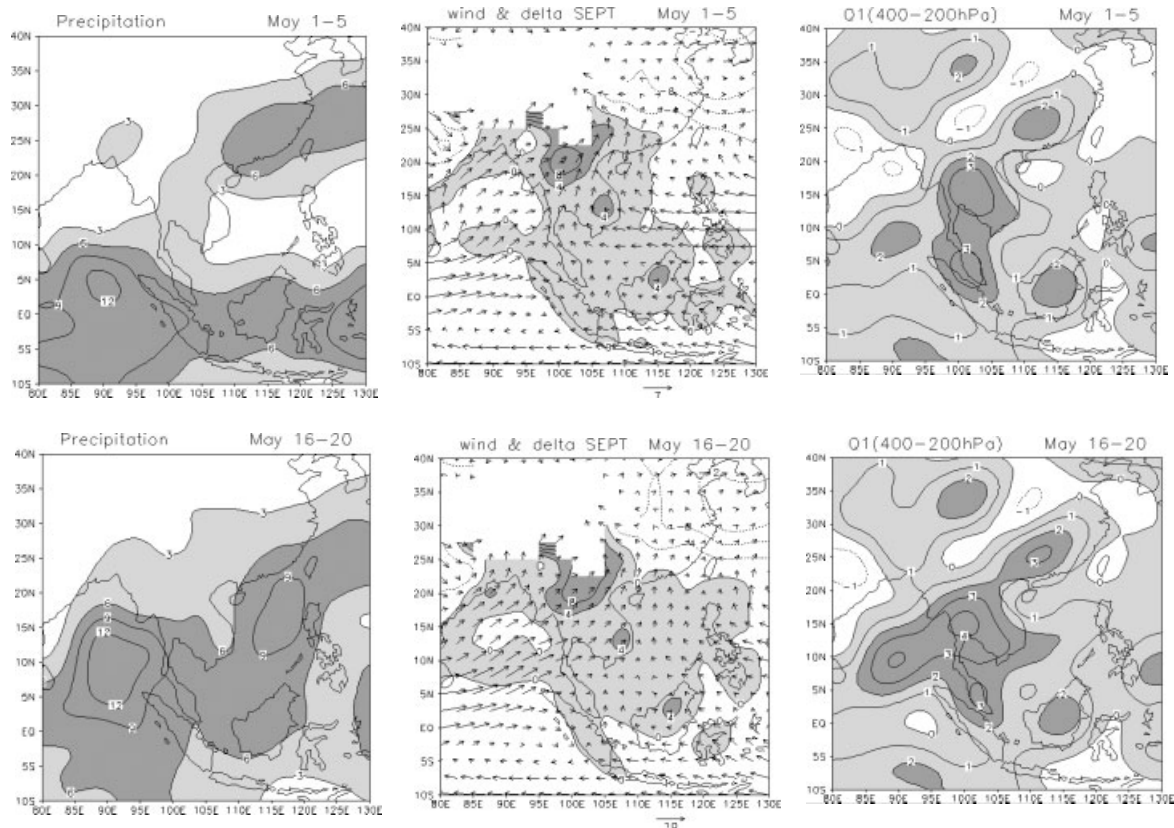


Figure 9. Evolution of precipitation rate (mm day^{-1} ; left column), 1000–850 hPa mean wind (arrows, m s^{-1}) and $\Delta\theta_{SE}$ (contour, $^{\circ}\text{C}$; middle column), and mean Q_1 ($^{\circ}\text{C day}^{-1}$) over 400–200 hPa (right column) from 1–5 May (top) to 16–20 May (bottom). Light and dark shadings in the left column denote values $>3 \text{ mm day}^{-1}$ and $>6 \text{ mm day}^{-1}$ respectively; those in the middle column are $>0^{\circ}\text{C}$ and $>4^{\circ}\text{C}$ respectively; those in the right column are $>0^{\circ}\text{C day}^{-1}$ and $>2^{\circ}\text{C day}^{-1}$ respectively. The distribution over regions higher than 2 km is excluded in the middle column

diabatic heating in the upper troposphere is much earlier and stronger over the Indochina Peninsula than over southern China, which influences the advance of the summer monsoon onset in these regions.

4.2. Propagation of the onset of the tropical ASM

The ASM onset is always accompanied by the occurrence of heavy rainfall, but the reverse not necessarily true. For instance, heavy rainfall over southern China commences on 1–5 May and even earlier (see Figure 9), but the ASM there has not started at that time. Thus, it seems that the ASM onset should not be determined only by rainfall or OLR, but be based on the establishment of a monsoon-related circulation, which is characterized by a change in the zonal vertical shear in accordance with the build-up of positive MGT. Based on this principle, it is proposed that the monsoon onset south of 20°N over the tropical Asian region must simultaneously meet the following two preconditions:

1. Establishment of a zonal vertical shear, with low-level (e.g. 850 hPa) westerlies and upper level (e.g. 200 hPa) easterlies.
2. A pentad mean OLR $< 240 \text{ W m}^{-2}$.

The selection of 240 W m^{-2} as the threshold is somewhat subjective. According to Wu and Wang (2000), it is approximately equivalent to a precipitation rate of 6 mm day^{-1} in the western North Pacific. It should

be pointed out that the above criteria only serve for the onset of tropical components of the ASM. As for the subtropical case, rainfall might still be a better choice.

Applying these two preconditions, the advance of the ASM onset in the tropical monsoon region is identified, pentad by pentad, from 1 May to 10 June (Figure 10). During the first pentad of May (Figure 10(a)), the summer monsoon is established only over Sumatra, although strong rainfall over $\sim 10 \text{ mm day}^{-1}$ occurs over the southern Indochina Peninsula and southern China. In the next two pentads, the tropical monsoon advances along the land bridge, first establishing over the southwestern Indochina Peninsula and then expanding to the entire southern peninsula. During the 16–20 May pentad (Figure 10(d)), the build-up of the summer monsoon is observed over the northern part of the land bridge. At the same time, the onset location extends into the central and southern SCS, accompanied by a rainfall of $>5 \text{ mm day}^{-1}$ over the entire SCS. In the next pentad, the onset expands quickly and almost covers the entire SCS (Figure 10(f)). On the other hand, the ASM also advances northwestward from the land bridge from early May, though somewhat slowly with respect to its northeastward advance, and covers the entire BOB by the end of May (Figure 10(g)), then over India and the eastern Arabian Sea on 10 June (Figure 10(h)).

These onset dates are similar to those from Lau and Yang (1997), who determined the onset based on changes in rainfall, but delayed by one to two pentads over the southern Indochina Peninsula. This difference is due to the delayed reversal from westerlies to easterlies at the upper levels relative to the occurrence of $>6 \text{ mm day}^{-1}$ rainfall. In this sense, the replacement of wintertime upper level zonal flow by its summertime counterpart appears to be a crucial precondition to determine the onset of the ASM. If only the occurrence of heavy rainfall was considered, then the ASM would have already been established over the entire Indochina Peninsula and southern China by the first pentad of May.

5. ROLE OF SURFACE HEAT FLUX

As discussed in Section 4, the ASM onset commences first over the southwestern Indochina Peninsula in early May, which is essentially ascribed to the establishment of southwesterlies over the BOB and its eastward extension, which is closely associated with the development of a cyclonic vortex over the BOB in April (see Figures 1 and 2). Thus, the origin of the cyclonic vortex over the BOB becomes a crucial factor for the ASM onset, which is addressed in this section.

The local heat forcing is believed to be a candidate for the establishment of the BOB vortex. Prior to and during the development of the cyclonic vortex over the BOB, strong sensible heat flux is found over the landmass west of the BOB. In particular, a maximum heating of up to $\sim 120 \text{ W m}^{-2}$ occurs over the entire Indian subcontinent rather than over the Tibetan Plateau (Figure 11(a)). On the other hand, the latent heating is quite weak over the Indian subcontinent, which is typical for the dry season there. Nevertheless, it reaches maxima over the ocean south of India and the Indochina Peninsula (Figure 11(b)). As a response, the cores of positive MGT are observed over the western BOB, India, the coastal region of the Arabian Peninsula and northern Africa (Figure 11(c)). The low-level warmest regions, represented by the northern boundary of positive MGT according to Equation (6), coincide geographically with the strong surface heat flux. This situation implies the dominant influence of the sensible heating on the low-level air temperature during the seasonal transition in the SAM regions. The distribution of pentad-mean time rate of change of 850 hPa geopotential height shows that the largest reduction of geopotential height by $\sim 40 \text{ gpm}$ per pentad not only occurs over the Indian subcontinent, but also over most of the BOB (Figure 11(d)). Such a local pressure reduction actually favours the development of the low-level depression and the mid-troposphere trough over the BOB.

It is noticed that the surface heat flux is not at its strongest over the BOB. Xu and Chan (2001) argued that the change in the thermal condition over the tropical Indian Ocean was mainly dominated by latent heat flux, the significant increase of which coincided with the onset of the 1998 ASM over the BOB in mid May. This implies that the local latent heating over the ocean likely contributes to the development of low-level cyclones during 26 April to 10 May. On the other hand, He *et al.* (2002) proposed another remote forcing mechanism using the complete form of the vorticity tendency equation (Wu *et al.*, 1999) to interpret the formation

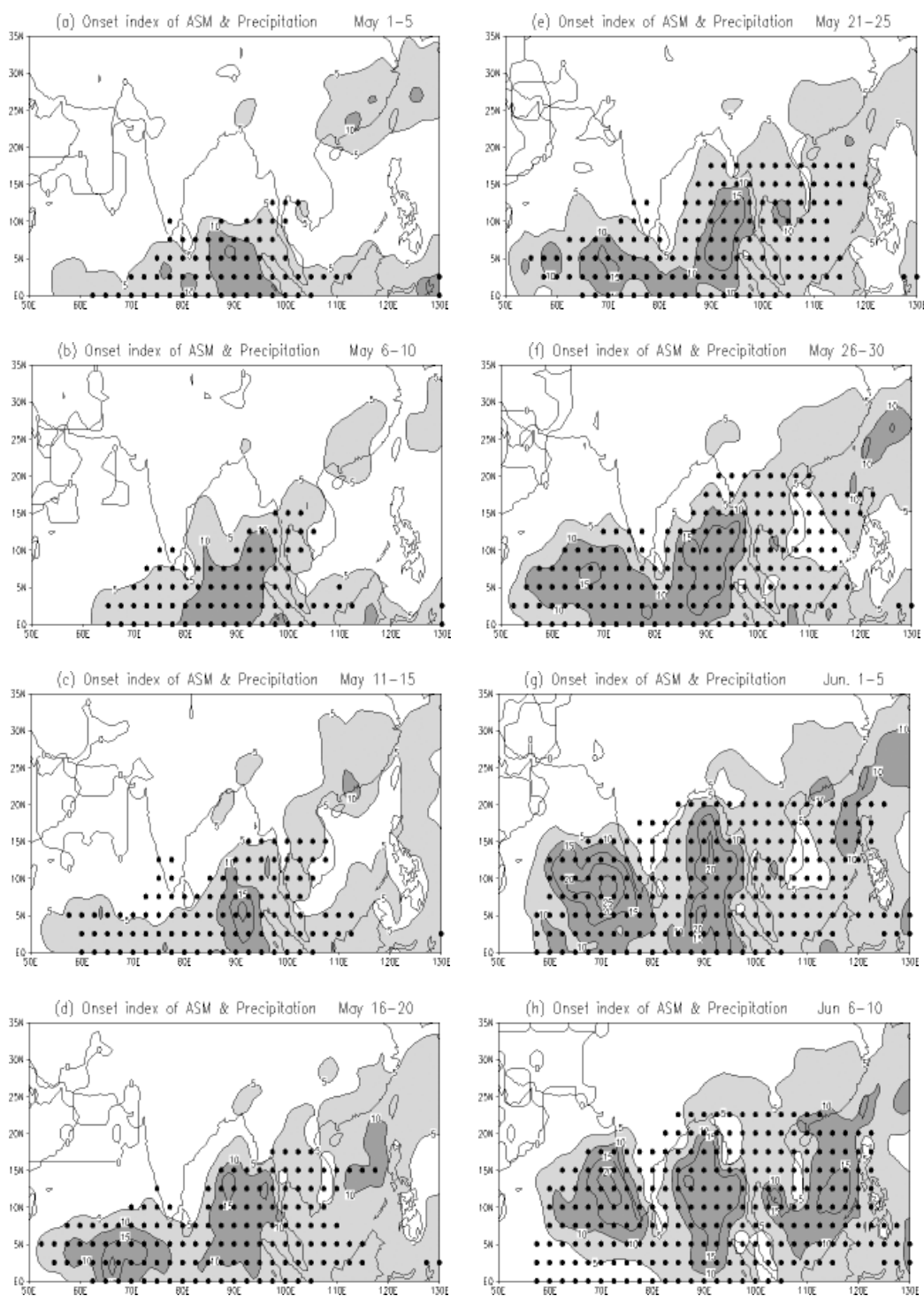


Figure 10. Climatological advance of the ASM onset denoted by closed circles and precipitation rate (mm day^{-1}) from 1-5 May (a) to 6-10 June (h) in sequence. Contour interval for precipitation rate is 5 mm day^{-1} , with light and dark shading indicating the values $>5 \text{ mm day}^{-1}$ and $>10 \text{ mm day}^{-1}$ respectively

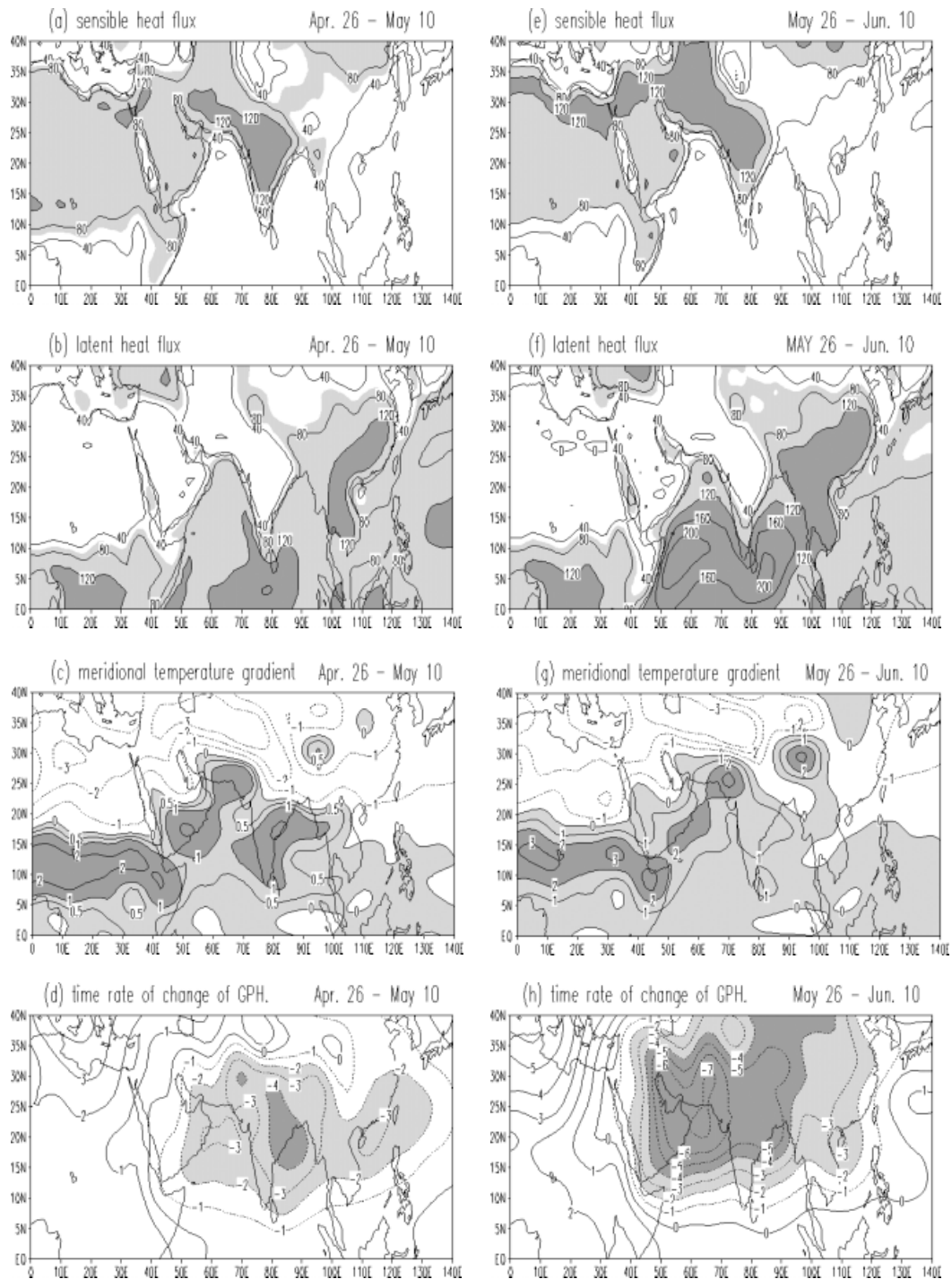


Figure 11. (a) and (e) Pentad mean sensible heat flux (W m^{-2}), (b) and (f) latent heat flux (W m^{-2}), (c) and (g) 850 hPa MGT ($^{\circ}\text{C}$ per 2.5° lat), and (d) and (h) time rate of change of geopotential height in each pentad (10 gpm) during 26 April–10 May (left column) and 26 May–10 June (right column). Light and dark shadings of heat flux indicate the values $>80 \text{ W m}^{-2}$ and $>120 \text{ W m}^{-2}$ respectively; those of the MGT in (c) $>0^{\circ}\text{C}$ per 2.5° lat and $>1^{\circ}\text{C}$ per 2.5° lat respectively; those of the MGT in (g) $>0^{\circ}\text{C}$ per 2.5° lat and $>2^{\circ}\text{C}$ per 2.5° lat respectively; those in (d) and (h) >20 gpm per pentad and >40 gpm per pentad respectively

and variation of the subtropical anticyclone in the Northern Hemisphere (Liu *et al.*, 2001). According to this theory, in a quasi-equilibrium state, the core of a mid or low level depression induced by the surface sensible heating tends to shift to the east of the heating centre. As for the case of latent heating, however, the counterpart emerges to the west. In this sense, the overlapping of thermal forcing effects originates from the intense sensible heating over India (Figure 11(a)); surface latent heating (Figure 11(b)) and condensation heating in the troposphere (Figure 9) over the Indochina Peninsula then account for the occurrence of the 850 hPa cyclonic vortex or the 500 hPa trough over the BOB. Therefore, it may be deduced that both the local and remote thermal forcing processes contribute to the development of the BOB cyclonic vortex.

Prior to and during the monsoon onset over the Indian subcontinent, the sensible heating over the Iranian Plateau, western Tibetan Plateau and surrounding regions undergoes a notable enhancement, while a weakening occurs over the Indian subcontinent (Figure 11(e)). At the same time, the latent heat flux over the Indian Ocean increases further (Figure 11(f)). These changes of surface heating lead to the maxima of positive MGT and the reduction in geopotential height to move from the BOB and India to the northern Arabian Sea and its adjacent landmass (Figure 11(g) and (h)), which favours the development of cyclonic circulations over these regions.

6. SUMMARY AND DISCUSSION

The climatological characteristics and evolution of the ASM onset over the tropical regions have been examined, with a focus on the corresponding physical processes and mechanisms responsible. The major conclusions can be summarized as follows.

Based on the 1979–95 mean pentad reanalysis data, development of cyclonic flow is first found over the BOB, and then over the northern SCS and the Arabian Sea during the seasonal transition period. It appears that this cyclonic flow plays a significant role in the ASM onset.

Although the atmosphere over the Indochina Peninsula has become quite thermally unstable since early April, the active convection there does not occur until the southwesterly flow associated with the cyclonic vortex over the eastern BOB converges with the southeasterlies from the WPSH over the SCS. The vertical profiles of Q_1 and Q_2 suggest that the latent heat released is transported to the upper troposphere by the cumulus- and turbulence-induced eddies in the convection, which results in the reversal of upper level MGT. As a response to this diabatic forcing, the wintertime MGGH at the upper levels reverses, which leads to the establishment of an easterly vertical wind shear. In this case, the ASM onset is completely accomplished over the Indochina Peninsula by mid May. Afterwards, with the eastward extension of the southwesterly flow and the retreat of the WPSH, onset occurs over the SCS in late May.

The strong ascending motion over the BOB to the SCS tends to sink preferentially over the desert of West Asia, giving rise to (adiabatic) warming in the upper troposphere and warming of the land surface due to the increase of clear-sky solar radiation. The former is responsible for the reversal of upper level MGT and the establishment of the Iranian high and the associated easterly flow. At the same time, the thermal forcing in the lower troposphere favours the development of a local thermal low or cyclonic vortex, which tends to induce and accelerate the westerly flow over the Arabian Sea. Through these processes, the ASM is set up over India by mid June.

Evidence shows that both the development of low-level cyclonic vortices over the western BOB and the reversal of the low-level MGT over South Asia are closely associated with the seasonal warming of the surface in southern Asia and the surrounding ocean. Further, the former not only seems to owe its existence to the increase in the local latent heat flux, but also relies on the remote thermal forcing, e.g. the condensation heating in the troposphere of the Indochina Peninsula and the sensible heating over India, whereas the latter appears to be more responsible for the sensible heat flux over the land of South Asia.

To summarize, the ASM onset can be described as a three-stage phenomenon, which was also proposed by Wu and Zhang (1998) and Chan *et al.* (2000) on the cases of 1989 and 1998 respectively. Details of the three stages are illustrated schematically in Figure 12, with each process or feature labelled by a letter in parentheses. In Stage I, increasing sensible and latent heat fluxes (a) lead to the development of a cyclonic

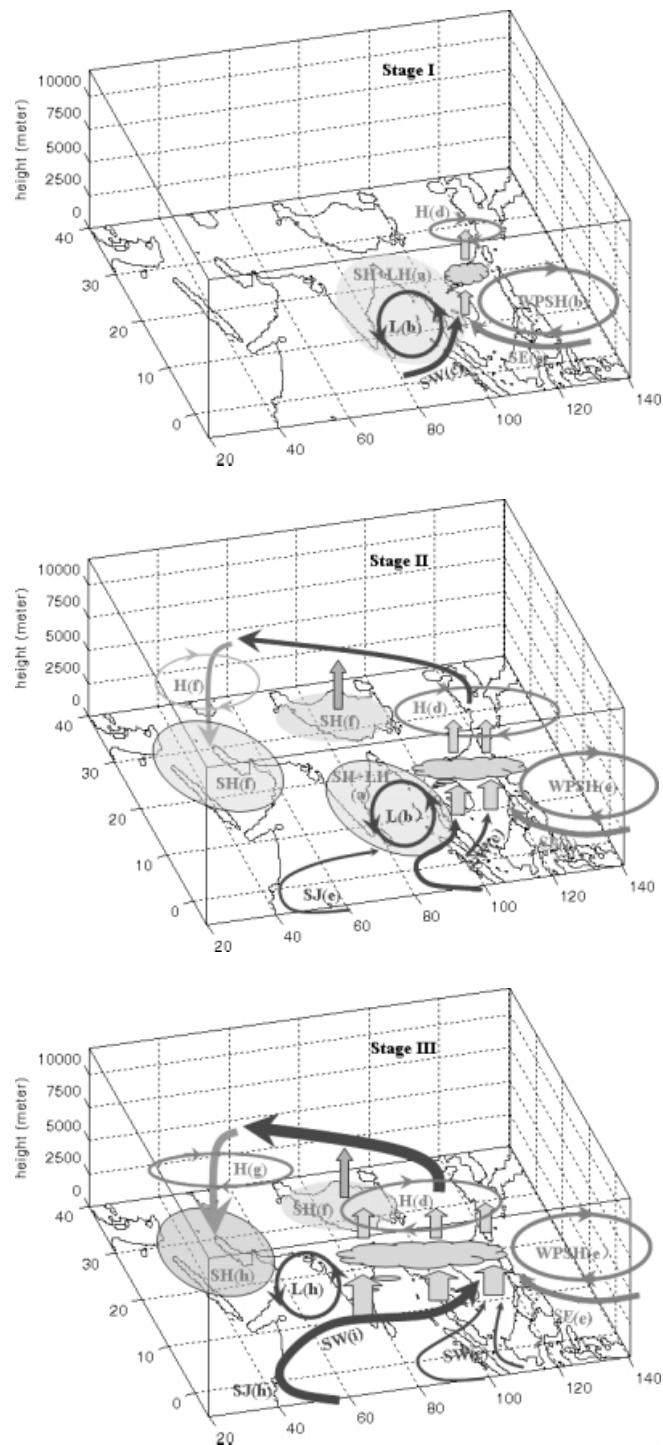


Figure 12. Schematic illustration of the advance of the tropical ASM onset. The meaning of abbreviations is as follows: SH+LH (surface sensible and latent heat fluxes), L (low-level low), SW (southwesterlies), SE (southeasterlies), WPSH (western Pacific subtropical high), H (upper level high), SJ (Somalia cross-equatorial jet). The occurrence sequence of the events is roughly indicated by the descending order of letters in parentheses. In general, the advance of the tropical ASM onset can be divided into three stages with time. Stage I (1 April–15 May) is the monsoon onset over the Indochina Peninsula; Stage II (16 May–25 May) is over the SCS; Stage III (26 May–15 June) is over the Arabian Sea and India. The northwest–southeast-oriented meridional circulation exists throughout the three stages

vortex (b) and increasing southwesterlies (c) over the BOB. Together with the southeasterlies (c) associated with the WPSH (b) over the SCS, the atmospheric stability over the Indochina Peninsula is reduced. The convergence of these two air streams gives rise to strong convection and an upper level warming-induced high (d). The ASM onset over the Indochina Peninsula is accomplished.

In Stage II, the eastward extension of southwesterlies over the Indochina Peninsula and the concurrent retreat of the WPSH (e) to the east of 120°E result in the prevalence of southwesterlies (e) and consequent active convection over the SCS, and hence the ASM onset over the SCS. Also, the Somali jet (e) is built up east of the eastern coast of Africa because of the rapid enhancement of the land–sea thermal contrast between the African continent and the Indian Ocean. At the same time, the thermal forcing of the eastern Tibetan Plateau (f) starts to work. The active convection over the BOB, the Indochina Peninsula and the SCS causes upper level subsidence over the Iranian desert and the Arabian Peninsula, which then leads to the development of the Iranian high (f) and an enhancement of surface sensible heat flux (f).

In Stage III, the northwest-oriented cell enhances. Together with the latent heat flux over the Arabian Sea, the intensified sensible heat flux (h) accelerates the development of low-level cyclonic vortex (h) over the east coast of the Arabian Peninsula, and then strengthens the related Somali jet (h) as well as southwesterlies (i) over the Arabian Sea. This situation triggers the ASM onset over India and the Arabian Sea.

This research presents only the long-term mean state for the ASM. However, the ASM has a large interannual variability in the onset date, place and triggering mechanism. Future research should investigate the individual cases of ASM onset and compare these with climatological results so as to improve our understanding for the ASM onset.

ACKNOWLEDGMENTS

We would like to thank the National Centers for Environmental Prediction and National Center for Atmospheric Research for providing the reanalysis data, the Climate Diagnostics Center for providing the OLR data, and the Climate Prediction Center for providing the Merged Analysis of Precipitation data. We would also like to thank Professor Wu Guoxiong and Dr Liu Yiming, of the Institute of Atmospheric Physics, Chinese Academy of Sciences, for their valuable suggestions and discussions. The comments and suggestions offered by two anonymous reviewers contributed to considerable improvements of the paper.

This research was sponsored by the City University of Hong Kong, grants 7010010 and 7001212.

REFERENCES

- Ananthakrishnan R, Pathan JM, Aralikatti SS. 1981. On the northward advance of the ITCZ and the onset of the southwest monsoon rains over the southeast Bay of Bengal. *Journal of Climatology* **1**: 153–165.
- Chan JCL, Wang YG, Xu JJ. 2000. Dynamic and thermodynamic characteristics associated with the onset of the 1998 South China Sea summer monsoon. *Journal of the Meteorological Society of Japan* **78**: 367–380.
- Chang C-P, Chen GT. 1995. Tropical circulation associated with the southwest monsoon onset and westerly surge over the South China Sea. *Monthly Weather Review* **123**: 3254–3267.
- Ding YH. 1994. *Monsoon over China*. Kluwer Academic Publishers.
- Ding YH, Xue JS, Wang SR, Chao QC, Sun Y, Liu YJ. 1999. The onset and activity of Asian monsoon and heavy flooding in China in 1998. In *Onset and Evolution of the South China Sea Monsoon and Its Interaction with the Ocean*, Ding Y-H, Li CY (eds). China Meteorological Press; 193–199.
- Flohn H. 1957. Large-scale aspects of “summer monsoon” in South and East Asia. *Journal of the Meteorological Society of Japan* (75th Ann. Vol.): 180–186.
- Flohn H. 1960. Recent investigation on the mechanism of the “summer monsoon” of southern and eastern Asia. In *Monsoons of the World*. The Manager of Publications: Delhi, India; 75–88.
- He H, McGinness JW, Song Z, Yanai M. 1987. Onset of Asian monsoon in 1979 and the effect of the Tibetan Plateau. *Monthly Weather Review* **115**: 1966–1995.
- He JH, Wen M, Shi XH, Zhao QH. 2002. Splitting and eastward withdrawal of the subtropical high belt during the onset of the South China Sea monsoon and their possible mechanism. *Journal of Nanjing University (Natural Sciences)* **38**: 318–330 (in Chinese).
- Hsu HH, Terng CT, Chen CT. 1999. Evolution of large-scale circulation and heating during the first transition of the Asian summer monsoon. *Journal of Climate* **12**: 793–810.
- Kalnay E, et al. 1996. The NCEP/NCAR 40-year reanalysis project. *Bulletin of the American Meteorological Society* **77**: 437–471.
- Krishnamurti TN. 1985. Summer monsoon experiment — a review. *Monthly Weather Review* **113**: 1590–1626.
- Krishnamurti TN, Ardanuy P, Ramanathan Y, Pasch R. 1981. On the onset vortex of the Asian summer monsoon. *Monthly Weather Review* **109**: 344–363.

- Lau KM, Yang S. 1997. Climatology and interannual variability of the Southeast Asian summer monsoon. *Advances in Atmospheric Sciences* **14**: 141–162.
- Lau KM, et al. 2000. A report of the field operations and early results of the South China Sea Monsoon Experiment (SCSMEX). *Bulletin of the American Meteorological Society* **81**: 1261–1270.
- Li C, Qu X. 1999. Characteristics of atmospheric circulation associated with summer monsoon onset in the South China Sea. In *Onset and Evolution of the South China Sea Monsoon and its Interaction with the Ocean*, Ding Y-H, Li CY (eds). China Meteorological Press; 200–209.
- Li C, Yanai M. 1996. The onset and interannual variability of the Asian summer monsoon in relation to land–sea thermal contrast. *Journal of Climate* **9**: 358–375.
- Liu YM, Wu GX, Liu H, Liu P. 2001. Dynamical effects of condensation heating on the subtropical anticyclones in the Eastern Hemisphere. *Climate Dynamics* **17**: 327–338.
- Luo H, Yanai M. 1983. The large-scale circulation and heat sources over the Tibetan Plateau and surrounding areas during the early summer of 1979. Part I: precipitation and kinematic analysis. *Monthly Weather Review* **111**: 922–944.
- Luo H, Yanai M. 1984. The large-scale circulation and heat sources over the Tibetan Plateau and surrounding areas during the early summer of 1979. Part II: heat and moisture budgets. *Monthly Weather Review* **112**: 966–989.
- Murakami T, Ding Y. 1982. Wind and temperature change over Eurasia during the early summer of 1979. *Journal of the Meteorological Society of Japan* **60**: 183–196.
- Matsumoto J. 1997. Seasonal transition of summer rainy season over Indochina and adjacent region. *Advances in Atmospheric Sciences* **14**: 231–245.
- Ramage CS. 1971. *Monsoon Meteorology*. Academic Press: New York.
- Rao YP. 1976. Southwest Monsoon. Meteorological Monograph, Synoptic Meteorology. No. 1, India Meteorological Department.
- Staff Member of the Academia Sinica. 1957. On the general circulation over eastern Asia (I). *Tellus* **9**: 432–446.
- Tao S, Chen L. 1987. A review of recent research on the East Asian summer monsoon in China. In *Monsoon Meteorology*, Chang C-P, Krishnamurti TN (eds). Oxford University Press; 60–92.
- Ueda H, Yasunari T. 1998. Role of warming over Tibetan Plateau in early onset of the summer monsoon over the Bay of Bengal and the South China Sea. *Journal of the Meteorological Society of Japan* **76**: 1–12.
- Webster PJ, Magana VO, Palmer TN, Shukla J, Tomas RA, Yanai M, Yasunari T. 1998. Monsoon process, predictability, and the prospects for prediction. *Journal of Geophysical Research* **103**: 14 451–14 510.
- Wu G, Zhang Y. 1998. Tibetan Plateau forcing and timing of the monsoon onset over South Asia and South China Sea. *Monthly Weather Review* **126**: 913–927.
- Wu GX, Liu YM, Liu P. 1999. The effect of spatially non-uniform heating on the formation and variation of subtropical high. I: scale analysis. *Acta Meteorologica Sinica* **57**: 257–263 (in Chinese).
- Wu R, Wang B. 2000. Interannual variability of summer monsoon onset over the western North Pacific and the underlying processes. *Journal of Climate* **13**: 2483–2501.
- Xie A, Liu X, Ye Q. 1996. Climatological feature of the South China Sea Monsoon onset. In *New Advance of Asian Monsoon Study*, He JH (eds). China Meteorological Press; 132–141 (in Chinese).
- Xu J, Chan JCL. 2001. First transition of the Asian summer monsoon in 1998 and the effect of the Tibet–tropical ocean thermal contrast. *Journal of the Meteorological Society of Japan* **79**: 241–253.
- Yan J. 1997. Climatological characteristics of southwesterly monsoon over the South China Sea. *Acta Meteorologica Sinica* **5**: 174–186 (in Chinese).
- Yanai M, Esbensen S, Chu JH. 1973. Determination of bulk properties of tropical cloud clusters from large-scale heat and source budgets. *Journal of the Atmospheric Sciences* **30**: 611–627.
- Yanai M, Li C, Song Z. 1992. Seasonal heating of the Tibetan Plateau and its effect on the evolution of the Asian summer monsoon. *Journal of the Meteorological Society of Japan* **70**: 319–351.
- Ye TZ, Gao Y-X. 1979. *The Meteorology of the Qianghai–Xizang (Tibet) Plateau*. Science Press (in Chinese).